

**Lama KHALIL, Thibault BRULÉ, and Ludivine FROMENTOUX**

HORIBA FRANCE SAS, 14 Boulevard Thomas Gobert - Passage Jobin Yvon, CS45002 - 91120 Palaiseau, France

**Abstract:** Stemming from the combination of Raman spectroscopy with optical microscopy, Raman microscopy has shown beyond doubt to be a key tool to probe the chemical structure of materials. Here, we use Raman imaging to investigate the chemical composition of a millimeter-sized core-shell  $\text{SiO}_2@ \text{TiO}_2$  bead. It is also shown that ViewSharp™ (optical topography imaging) in combination with SmartSampling™ (which uses white light image contrast variations to optimize Raman mapping) is able to efficiently assess the uniformity of the  $\text{TiO}_2$  shell layer covering the  $\text{SiO}_2$  surface. In this case, equivalent information was acquired 50 times faster than by conventional Raman imaging.

**Keywords:** Raman microscopy, Core-shell bead, Chemical characterization, SmartSampling™.

## Introduction

In recent years, core-shell particles have attracted significant attention due to their smart properties, resulting from their unusual composition compared to other particle types. These structures combine two or more different material layers; the inner particle is the core, encapsulated by other outer layers called the shell [1,2]. Size, morphology, and composition are the key features that strongly affect the performance and suitable applications of such structures. Thus, several investigations have focused on the characterization of their chemical composition. However, this remains particularly challenging for millimetre-sized core-shell spheres, which require long measurement times for their study, due to the high spatial resolution needed to characterize small features typically found on such particles.

In this application note, we study the chemical composition of a silica ( $\text{SiO}_2$ ) bead, having a diameter of about 1.7 mm, coated with a layer of titania ( $\text{TiO}_2$ ).  $\text{TiO}_2$  exists in three different polymorphs, namely anatase, rutile and brookite [3]. Among the three, anatase is the most extensively employed in many applications, including photocatalysis and photoelectrocatalysis. In this respect, the precise experimental determination of the  $\text{TiO}_2$  polymorph is sorely needed for the potential applications of  $\text{TiO}_2$ -coated beads. Indeed, Raman microscopy has proven to be a powerful technique providing information on the chemical structure, polymorphism and much more. Here, by using this technique, we present a detailed characterization of the chemical content, spatial distribution of components, and uniformity of the  $\text{TiO}_2$  shell layer within the core-shell  $\text{SiO}_2@ \text{TiO}_2$  bead. We also compare SmartSampling™ [4,5], the new HORIBA tool for Raman imaging, to the conventional point-by-point acquisition mode to show how SmartSampling™ combines speed and accuracy to offer fast Raman maps for such large-area samples.

## Instrument and methods

The micro-Raman measurements were performed using the confocal HORIBA LabRAM Soleil™ (Figure 1), offering full automation. A 532 nm laser excitation was focused down to a micrometric spot on the sample surface through a 50x ELWD visible objective lens (NA = 0.6; 11 mm long working distance). The Raman spectra were measured using a spectrometer with a 600 gr/mm grating and a laser power of 48 mW at the sample. The LabRAM Soleil™ instrument was directly controlled by LabSpec6 software.

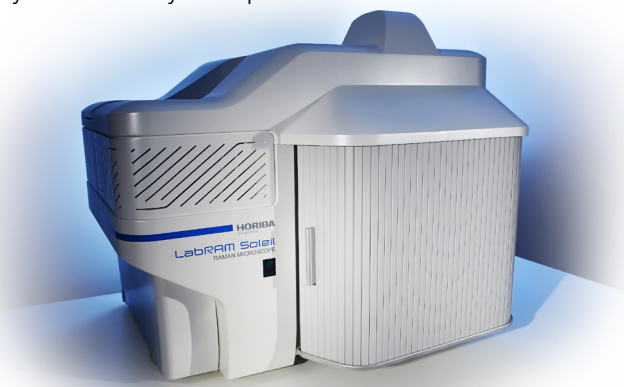


Figure 1: The confocal HORIBA **LabRAM Soleil™** Raman microscope.

A 3D topography image of the bead was constructed using the ViewSharp™ application, in which all surfaces are in focus simultaneously. This topography was extracted and then used during the Raman acquisition.



For fast and efficient Raman mapping, Raman measurements were conducted using the SmartSampling™ image acquisition, allowing large areas to be acquired in a fraction of the time required with the standard point-by-point mapping mode. SmartSampling™, exclusive to the LabRAM Soleil™, selects the location of acquisition points of a Raman map according to their relevance rather than following the typical square with repetitive positions. Based on the video image, the SmartSampling™ algorithm automatically defines an optimum path to reduce the total measurement time. This tool intelligently combines precision with high speed.



## Results

Two Raman maps were acquired using the standard point-by-point mapping mode (Figure 2a) and SmartSampling™ (Figure 2b) on a large area of the bead ( $600 \times 700 \mu\text{m}^2$ ). To resolve the different component spectra and their spatial distribution, a multivariate data analysis was applied on both maps. The data analysis process was divided into three main parts: (i) preprocessing of the raw spectral data, aiming at removing the background (i.e., baseline correction) and then at normalizing the spectra to ease access to the relevant information, (ii) manual determination of the reference spectra and their identification with the KnowItAll® database (i.e., multivariate data analysis), and (iii) post-processing of the image.

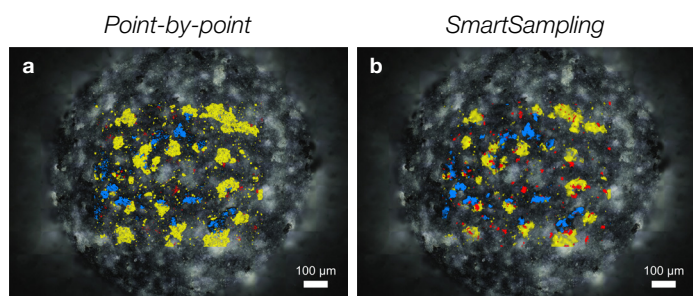


Figure 2: Two Raman maps superimposed on the same optical image. These maps have been obtained via two distinct acquisition modes: **a** the standard point-by-point mapping mode (26h40min), and **b** SmartSampling™ (1h10min). Transparent, blue, red, and yellow colors correspond to pure anatase  $\text{TiO}_2$ , amorphous  $\text{SiO}_2$ , quartz and carbon, respectively.

Four compounds were identified, namely pure anatase  $\text{TiO}_2$  (shown as transparent, as it covers most of the  $\text{SiO}_2$  surface), amorphous  $\text{SiO}_2$  (blue), quartz (red), and carbon (yellow). This chemical analysis unambiguously determines the  $\text{TiO}_2$  polymorph as pure anatase. It also shows that  $\text{SiO}_2$  exists in both amorphous and crystalline (quartz) forms. In Figure 2, we present the distribution of these compounds across the mapped region. As observed from the Raman map, the  $\text{TiO}_2$

coating is non-uniform, as it does not cover the entire  $\text{SiO}_2$  surface. This non-uniformity could be due to an insufficient amount of  $\text{TiO}_2$  to cover the whole surface of the bead during sample preparation. Figure 2 also compares two distinct mapping modes, the standard point-by-point acquisition mode with SmartSampling™. Although the Raman map of Figure 2a has been acquired with better spatial resolution than that of Figure 2b, the comparison between both maps reveals that they look nearly identical. This indicates that SmartSampling™ provides high-resolution Raman images with essentially equivalent information content. Additionally, the total measurement time with SmartSampling™ (1h10min) is significantly decreased compared to the standard map (26h40min). Thus, SmartSampling™ acquires high-resolution images in a fraction of the time needed for conventional maps (here, 50x faster than the point-by-point mapping mode). Consequently, this tool is ultimate to obtain fast Raman maps for millimetre-sized spheres.

## Conclusion

To conclude, Raman microscopy is a powerful technique that retains the advantages of Raman spectroscopy through compound identification, but also adds those of imaging via the determination of the spatial distribution of these compounds. By using this technique, we have successfully studied the chemical composition of a millimetre-sized core-shell  $\text{SiO}_2@ \text{TiO}_2$  bead. Our results show that the  $\text{TiO}_2$  coating exhibits an anatase crystal phase and forms a non-continuous layer on top of the  $\text{SiO}_2$  surface. Thanks to SmartSampling™, Raman imaging of such large-area specimens have become faster, as this imaging tool quickly identifies key information while maintaining high spatial resolution.

## References

1. R. Hayes, A. Ahmed, T. Edge, and H. Zhang. Core-shell particles: Preparation, fundamentals and applications in high performance liquid chromatography. *J. Chromatogr. A* 1357, 36-52 (2014).
2. R. Ghosh Chaudhuri and S. Paria. Core/Shell Nanoparticles: Classes, Properties, Synthesis Mechanisms, Characterization, and Applications. *Chem. Rev.* 112, 2373-2433 (2012).
3. M. Landmann, E. Rauls, and W. G. Schmidt. The electronic structure and optical response of rutile, anatase and brookite  $\text{TiO}_2$ . *J. Phys.: Condens. Matter* 24, 195503 (2012).
4. T. Brulé, L. Fromentoux, A. Holland, and S. Laden. A Revolution in Raman Imaging. *Spectroscopy*, 54-57 (2021).
5. S. Desplanche, T. Brulé, and C. Eypert. Characterization of protective mask fibers by Raman microscopy. Horiba Scientific (2021).

info.sci@horiba.com

**USA:** +1 732 494 8660  
**UK:** +44 (0)1604 542 500  
**China:** +86 (0)21 6289 6060  
**Taiwan:** +886 3 5600606

**France:** +33 (0)1 69 74 72 00  
**Italy:** +39 06 51 59 22 1  
**India:** +91 (80) 4127 3637  
**Brazil:** +55 (0)11 2923 5400

www.horiba.com/scientific

**Germany:** +49 (0) 6251 8475 0  
**Japan:** +81(75)313-8121  
**Singapore:** +65 (6) 745-8300  
**Other:** +33 (0)1 69 74 72 00